ELECTROCHEMICALLY ASSISTED LEACHING FOR METAL RECOVERY FROM LUNAR REGOLITH

Caroline G. Morin[1], Amelia Preble[1], Geoffrey M. Geise (advisor)[1]
[1]Department Chemical Engineering, University of Virginia

Abstract

In-situ resource utilization (ISRU) enables sustained human presence in space by leveraging local materials. Lunar regolith, the fine particulate covering the Moon's surface, contains valuable resources including oxygen, water, metals (Al, Fe, Ti), silicon, and ceramics. This study investigates a novel electrochemically assisted leaching method selective metal extraction from lunar regolith with minimized reagent consumption. A three-chamber electrochemical cell incorporating a bipolar membrane and an anion exchange membrane was designed to generate acid and regenerate reductant in situ. Anorthosite, the most abundant mineral in the lunar highlands, was selected as a model substrate to evaluate aluminum extraction. Ex-situ hydrochloric acid leaching experiments were conducted over a range of temperatures (40-80°C), duration (0.5 to 7 hours), and acid concentration (0.01-1M) to establish baseline dissolution behavior. Aluminum concentrations in leachate samples were quantified via spectrophotometric analysis. Results indicate that while increasing the temperature and acid concentration enhances aluminum dissolution, appreciable dissolution can still be achieved at reduced temperature (40°C) and low acid concentrations. Proof-of-concept operation of the electrochemical cell demonstrates its ability to achieve these conditions through in situ acid generation, supporting the feasibility of electrochemical reagent regeneration for lunar ISRU applications.

1. Background

1.1 In Situ Resource Utilization

In situ resource utilization (ISRU) refers to the practice of using local resources to support human life and operations in space. Both sustained lunar presence and deep space exploration missions benefit from the ability to source and manufacture materials on demand due to limited resupply options and uncertainty in mission needs[1]. ISRU significantly reduces dependency on transporting materials from Earth, thereby lowering mission cost, risks, and reliance on terrestrial supplies[2]. Current ISRU efforts focus on developing novel technologies to characterize, extract, and refine lunar resources for essential products such as rocket propellants, fuel cell reactants, materials for infrastructure, and life support consumables. While progress has been made towards advancing some mining pathways, particularly for water and O_2 extraction, there remains a critical gap in translatable methods for metal and metalloid recovery from lunar regolith[3].

1.2 Composition of Lunar Regolith

Lunar regolith is a layer of dust, soil and fragmented rock on the surface of the Moon[4]. Regolith consists primarily of minerals such as anorthosite, pyroxene, olivine, and ilmenite, with absolute and relative abundances varying depending on the location[5]. The surface of the Moon is characterized by two primary regions based on geological history and regolith composition: the highlands and the maria. The highlands are predominantly composed of anorthosite, light colored, calcium rich minerals, while the maria consist primarily of darker, iron- and magnesium-rich basalts[4]. The bulk chemical composition of highland and maria regolith are summarized in *Table 1.* While each region exhibits a distinct overall composition, they are mixtures of the same minerals simply expressed at different ratios[6]. Thus, mining technologies that are resilient to variation in composition and validated

common lunar minerals could be broadly applied across multiple regions of the Moon.

***Table 1**: Bulk chemical compositions of highland and maria regolith (Taylor, 1975)[7]. These compounds exist in mineral and amorphous phases rather than pure oxides.*

Compound	Composition	
	Maria	Highlands
SiO_2	45.4%	45.5%
Al_2O_3	14.9%	24.0%
CaO	11.8%	15.9%
FeO	14.1%	5.9%
MgO	9.2%	7.5%
TiO_2	3.9%	0.6%
Na_2O	0.6%	0.6%
Total	99.9%	100%

There is strong interest in refining lunar regolith to generate purified resources including oxygen, water, metals (Al, Fe, Ti), metal alloys, silicon, and ceramics[2]. To date, ISRU technologies have primarily focused on oxygen recovery, often producing metal alloys and unreacted slag as byproducts that require further processing[8–10]. As efforts towards sustained lunar presence advance, more sophisticated mineral extraction and metal production processes designed with end-use in mind are required[11].

1.3 Conventional Metal Extraction

Mining technologies for ISRU must also be tailored to the lunar environment. Natural factors such as low gravity, extreme temperatures, and ultra-high vacuum, along with operational constraints like limited human access and resource availability, must be considered when choosing materials and strategies. Ideal systems would achieve high throughput, require minimal reagents, operate with low energy input, and leverage the lunar environment when possible[1,11]. Given these specifications, terrestrial mining systems do not translate to the lunar environment without significant modification. However, recent advances in terrestrial mining technologies may be adaptable to ISRU applications[12]. Global decarbonization is driving surging demand for critical energy materials and novel sustainable manufacturing[13]. Further, traditional high-grade deposits have become depleted, necessitating more efficient extraction techniques and sourcing from more dilute resources[12,14]. In other words, terrestrial mining is now developing technology to recover metals from novel sources with higher efficiency and a fraction of consumed resources.

Two of the most commonly employed methods to extract metals from ores are hydrometallurgy, which uses aqueous solutions to dissolve and recover metals, and pyrometallurgy, which applies heat to melt ores and removes metals in molten form[15]. While many metallurgical processes combine both approaches, final purification and recovery steps for high-purity metal products are typically hydrometallurgical[16]. Advantages of hydrometallurgy for metal recovery include high recovery efficiencies for a broad range of metals, ability to achieve high purity products, and low energy consumption. In addition, the field of hydrometallurgy is committed to establishing ‘circular hydrometallurgy’ or the design of energy-efficient and resource-efficient processes that consume minimum quantities of reagents and result in minimum waste[13]. A standard hydrometallurgical process consists of three main steps: leaching of metal from ore into solution, purification of the solution to remove impurities, and recovery of the metal in either a salt or pure metal form[17]. Leaching of metal oxides commonly employs high concentrations of strong acids (e.g. HCl or H_2SO_4) in combination with hydrogen peroxide (H_2O_2) as a chemical reductant[18]. However, H_2O_2 decomposes upon reaction, requiring large quantities of the reagent to sustain the process. These limitations highlight the need for alternative extraction strategies that minimize reagent consumption while

maintaining process efficiency under lunar constraints[13].

1.4 Electrochemically Assisted Leaching

Electrochemically assisted leaching offers a promising pathway to address these challenges by enabling in situ reagent generation. Electrochemical systems can directly produce H^+, allowing for controlled acid generation and reducing reliance on externally supplied reagents[19,20]. This approach enables dynamic tuning of leaching conditions while minimizing reagent consumption. In addition, electrochemical methods allow for regeneration of redox-active species; for example, iron (Fe^{2+}) can be continuously regenerated via reduction at the cathode and used as a redox mediator in leaching processes[21,22]. Therefore, the central hypothesis of this work is that reducing the reagent demands of conventional leaching through an electrochemical regeneration could enable viable in-situ metal extraction from lunar regolith.

Electrochemically assisted leaching can be realized using either a two- or three-chamber configuration, depending on whether a reducing agent is required. In the two-chamber cell, H^+ is generated at a bipolar membrane (BPM) interface through water splitting and transported into the cathode chamber containing the mineral slurry[19]. Here, the acidic environment promotes metal dissolution while any spent reducing agent Fe^{3+} is electrochemically reduced back to Fe^{2+} at the cathode, a strategy demonstrated by Diaz et al. (2018) for lithium-ion battery recycling[18]. While this configuration enables simultaneous acid generation and reductant regeneration, a three-chamber cell was implemented in this study to isolate and optimize acid generation.

In the three-chamber system (*Figure 1*), the mineral slurry is placed in a center chamber, separated from the cathode by an anion exchange membrane (AEM) to prevent H^+ reduction at the cathode[23]. H^+ generated at the BPM is transported into the center chamber, establishing the acidic conditions required for leaching[19,20]. At the cathode, water reduction produces H_2 and OH^- (*Equation 1*), contribution to local charge balance and completing the electrochemical circuit[24]. A supporting electrolyte, NaCl, is added to the catholyte to facilitate Cl^- transport across the AEM, maintaining electroneutrality and improving dissolution efficiency[25]. While NaCl introduces an additional material, it is not consumed and can be recovered and recirculated after metal precipitation[26,27]. In the anode chamber, the OH^- generated at the BPM is oxidized to produce O_2 and water (*Equation 2*)[19,20,24]. An inert electrolyte, Na_2SO_4, is used in the anode chamber and a supporting electrolyte, NaCl, is added to the center chamber to enhance conductivity and avoid the formation of reactive species. These electrolyte selections are specific to laboratory testing and are not intrinsic to practical ISRU system design. This electrochemical configuration enables controlled acid generation within the leaching environment and forms the basis for the experimental system evaluated in this study.

$$2e^- + 2H_2O \rightarrow 2OH^- + H_2 \quad \textbf{(1)}$$
$$E^\circ = -0.83\ V$$

$$4OH^- \rightarrow O_2 + 2H_2O + 4e^- \quad \textbf{(2)}$$
$$E^\circ = 0.401\ V$$

2. Methods

2.1 Mineral Selection

Anorthosite, specifically the anorthite endmember ($CaAl_2Si_2O_8$), was selected as the mineral of interest for this study. Anorthite does not require a reducing agent for Al^{3+} extraction and is abundance in the lunar south pole, the target region of the Artemis program and a

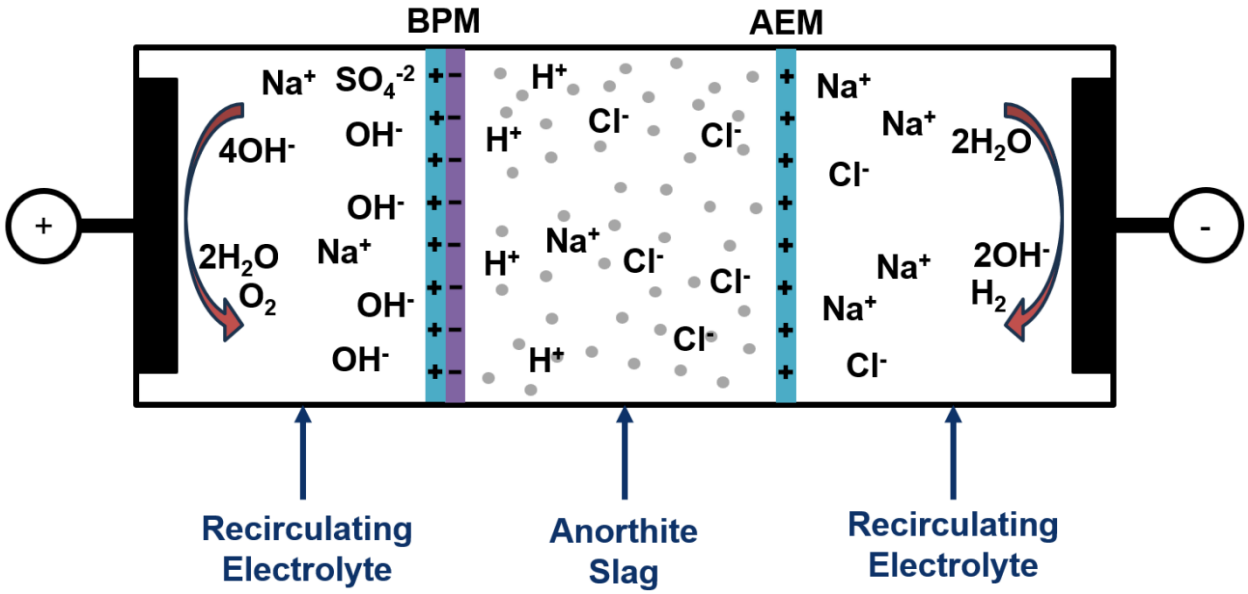

***Figure 1*: Schematic of the Three-Chamber Electrochemical Cell** – *Electrochemical cell used in this study for acid generation and mineral leaching. A bipolar membrane (BPM) operated in reverse bias generates H^+ and OH^- via water dissociation. H^+ is transported into the center chamber containing the anorthite slurry, enabling acid-driven dissolution, while OH^- migrates to the anode chamber and is oxidized to O_2. An anion exchange membrane (AEM) separates the center and cathode chambers, allowing Cl^- transport to maintain charge balance while preventing reduction of H^+ at the cathode. Supporting electrolytes are recirculated in the outer chambers to sustain conductivity and enable continuous operation.*

likely site for future resource recovery[28,29]. The material was sourced from Space Resource Technologies as a lunar regolith simulant representative of highland compositions. The simulant is composed primarily of crystalline anorthite with minor secondary phases, consistent with reported lunar highland mineralogy. Detailed compositional and structural characterization of the material, including phase composition and elemental analysis, is provided by the supplier.

The material was used as received without further modification or pretreatment.

2.2 Ex Situ Leaching Experiments

Ex situ leaching experiments were conducted in batch mode to evaluate the dissolution of aluminum from anorthite under varying acid concentrations and temperatures. In all experiments, 2 g of anorthite was added to 100 mL of hydrochloric acid (HCl) solution, corresponding to a solid-to-liquid ratio of 20 g/L. The HCl solution was prepared using ACS-grad HCl (Sigma-Aldrich) and deionized (DI) water.

Leaching experiments were performed at 40°C and 80°C. The higher temperature condition (80°C), also at 3M HCl, was used to establish a benchmark for dissolution under favorable kinetic conditions, while 40°C was selected to reflect the maximum operating temperature of the bipolar membrane used in the electrochemical system[30,31]. At 40°C, three acid concentrations (0.1M, 1M, and 3M HCl) were tested to evaluate the minimum acid conditions required for Al^{3+} dissolution. These conditions were selected to establish the range of acid concentrations relevant to electrochemical operation, where H^+ is generated dynamically rather than maintained at a fixed concentration. Experiments were conducted in sealed glass vessels placed in a temperature-controlled silicone oil bath and continuously stirred using a magnetic stir bar to maintain suspension of

solid particles. Aliquots (2 mL) were collected at specified time intervals (1, 7, and 20 hours) for analysis. Initial aliquots contained both solid and liquid phases; however, subsequent samples were filtered using a 0.45 µm syringe filter to isolate the liquid phase prior to analysis.

At the conclusion of each experiment, the remaining solid material was separated from the leachate by centrifugation. The recovered solids were dried in a convection oven followed by vacuum drying prior to storage for future characterization. Final solution pH was recorded for selected experiments to assess acid consumption relative to stoichiometric requirements for complete dissolution.

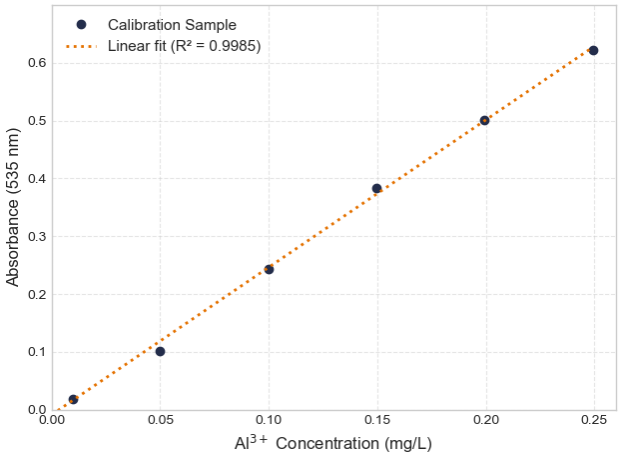

Figure 2: ECR Complex Calibration Curve *- Calibration curve relating absorbance to Al^{3+} concentration for the Al^{3+}–ECR complex at 535 nm. The linear relationship demonstrates consistency with Beer's Law over the measured range.*

2.3 Aluminum Characterization

Aluminum concentrations in leachate samples were determined using a colorimetric method based on complexation with Eriochrome Cyanine R (ECR). In this method, Al^{3+} forms a colored complex with ECR under buffered conditions, and the resulting absorbance is measured using UV–Vis spectroscopy at 535 nm. Detailed reagent preparation and procedure are described in *Standard Methods for the Examination of Water and Wastewater*[32,33].

The concentration of Al^{3+} can be determined using Beer's Law, which relates absorbance to concentration through the interaction of light with the Al–ECR complex. As the concentration of the colored complex increases, a greater fraction of incident light is absorbed, resulting in a proportional increase in measured absorbance. A calibration curve (*Figure 2*) was developed using aluminum standard solutions spanning the expected concentration range of the leachate samples, and linearity was confirmed prior to analysis.

While this method provides reliable quantification of Al^{3+}, the presence of coexisting ions may influence complex formation and were therefore evaluated. Because anorthite contains calcium and aluminum at a Ca:Al ratio of 1:2, potential interference from Ca^{2+} complexation with ECR was assessed using solutions with varying Ca:Al ratios (1:1, 10:1, and 100:1) under both low and high total dissolved solids (TDS) conditions. No significant interference from Ca^{2+} was observed, confirming that aluminum concentrations could be reliably quantified under the experimental conditions.

2.4 Electrochemical Cell Design and Testing

Electrochemical experiments were conducted to evaluate H^+ generation in the center chamber in the absence of solid material. A three-chamber electrochemical cell was constructed with an anode chamber (100 mL), center chamber (28 mL), and cathode chamber (100 mL), separated by a BPM and an ammonium-functionalized styrene–divinylbenzene AEM, both with polyester reinforcement. The anolyte consisted of 0.5M Na_2SO_4 and the center chamber and the catholyte contained 1M NaCl. The active area of the BPM and AEM were each 1.77 cm^2 (1.5 cm diameter), and the membranes were obtained from PCA

(PCCell)[31]. The BPM was operated in reverse bias and has a high current efficiency for water splitting (>95%).

Nickel foil electrodes (1.5 cm diameter, 0.3 mm thickness) were used for both the anode and cathode. The cell was operated galvanostatically at a current density of 50 mA/cm^2 and cell voltage was recorded continuously during operation[19].

The anode and cathode chambers were mixed using overhead stirrers, while the center chamber was stirred using a magnetic stir bar to ensure uniform solution conditions. The cell was maintained at 40°C using a temperature-controlled water bath to match the operating constraints of the bipolar membrane.

The pH of the center chamber was monitored over time using a Mettler Toledo pH probe and compared to theoretical predictions based on the applied current. These experiments were used to assess the capability of the system to achieve target acid concentrations for future leaching applications.

3. Results & Discussion

3.1 Ex Situ Leaching

The dissolution of aluminum from anorthite was evaluated as a function of acid concentration, temperature, and time. *Figure 3* shows the fraction of aluminum leached as Al^{3+} over time for varying HCl concentrations at 40°C, along with high HCl concentration at 80°C. Aluminum yield is defined as the fraction of total aluminum in the initial anorthite that is recovered as dissolved Al^{3+} in solution.

A strong dependence of dissolution behavior on both acid concentration and temperature was observed. At 40°C, increasing the HCl concentration from 0.1M to 3M resulted in a substantial increase in aluminum yield, with final extraction increasing from approximately 20% to over 60% after 20 hours. This behavior can be understood from the stoichiometry of anorthite dissolution, which requires multiple equivalents of protons:

$$CaAl_2Si_2O_8 + 8H^+ \rightarrow Ca^{2+} + 2Al^{3+} + 2SiO_2 + 4H_2O \quad \textbf{(3)}$$

Based on this reaction, complete dissolution of anorthite at a solid loading of 20 g/L requires a minimum acid concentration of approximately 0.17 M. As a result, the 0.1 M condition is inherently limited by proton availability and cannot achieve full aluminum extraction. The observed yields approaching ~20% under these conditions are therefore consistent with stoichiometric constraints rather than kinetic limitations[34,35].

In addition to this stoichiometric requirement, previous studies have reported a reaction order of 1.5 with respect to H^+ concentration, indicating that dissolution rates increase nonlinearly with increasing acid concentration[34]. Temperature also had a pronounced effect on dissolution kinetics. At 3M HCl, increasing the temperature from 40°C to 80°C resulted in near-complete aluminum

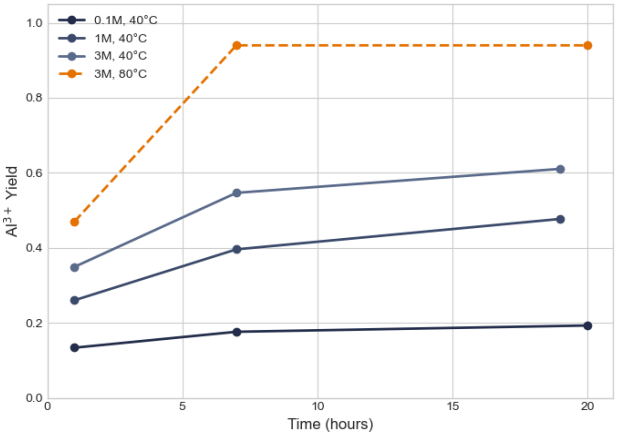

Figure 3: Al^{3+} Yield vs. Time *- Al^{3+} yield (fraction of total aluminum dissolved from anorthite) as a function of time for varying HCl concentrations and temperatures.*

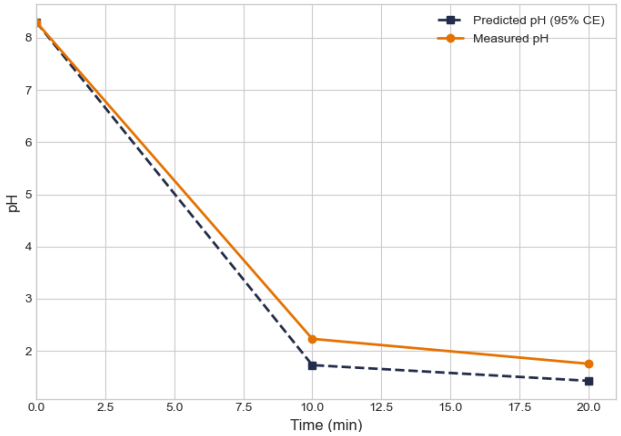

Figure 4: Predicted vs. Measured pH *- Measured and predicted pH in the center chamber as a function of time during electrochemical operation. Predicted values were calculated based on Faraday's law of electrolysis assuming 95% current efficiency for water dissociation at the bipolar membrane (BPM) and the same starting pH.*

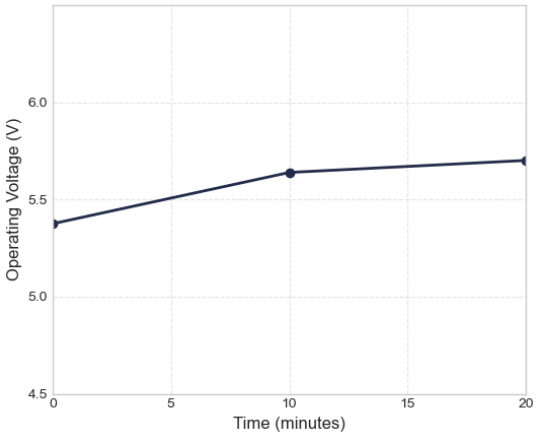

Figure 5: Operating Voltage vs. Time *- Cell voltage as a function of time during electrochemical acid generation in the three-chamber cell. The relatively stable voltage (5.4–5.7 V) indicates consistent electrochemical performance under galvanostatic operation.*

extraction (~95%) within 7 hours, compared to significantly lower yields at 40°C. This behavior is consistent with Arrhenius-type kinetics, where increased temperature enhances reaction rates by lowering the effective activation barrier[30].

Importantly, measurable aluminum dissolution was observed even under low acid concentration (0.1M) and moderate temperature (40°C), demonstrating that leaching can proceed under relatively mild conditions. This result is particularly significant for electrochemical applications, where acid is generated in situ and may not reach high bulk concentrations. These findings highlight the importance of balancing acid generation and consumption in electrochemical systems to achieve efficient metal extraction.

3.2 Electrochemical Cell Testing

The performance of the electrochemical cell was evaluated by comparing experimentally measured pH in the center chamber to values predicted from applied current. The predicted pH was calculated based on Faraday's law of electrolysis assuming 95% current efficiency for water dissociation at the BPM. *Figure 4* shows the measured and predicted pH as a function of time.

The pH decreased from near-neutral conditions to approximately pH 2 within 10 minutes of operation, demonstrating rapid acidification of the solution. The cell voltage (*Figure 5*) remained relatively stable during operation, increasing only slightly from approximately 5.4 to 5.7 V over 20 min, indicating consistent electrochemical performance during acid generation.

Good agreement between predicted and measured values was observed, indicating that H^+ generation in the center chamber proceeds close to the expected rate. The slight deviation between predicted and measured values may be attributed to partial crossover of OH^- across the AEM, or non-ideal selectivity between competing anions[23].

These results confirm that the electrochemical system can generate acid in situ at rates consistent with theoretical predictions. When considered alongside the ex situ leaching results, this acid generation rate is sufficient to achieve measurable aluminum dissolution. Future work will incorporate anorthite directly into the center chamber to evaluate leaching under dynamically generated acid conditions.

4. Conclusion

This study demonstrates the feasibility of electrochemically assisted leaching for selective metal extraction from lunar regolith analogs. Ex situ experiments demonstrated that aluminum dissolution from anorthite is strongly dependent on acid concentration and temperature, with higher H^+ availability significantly enhancing extraction. Importantly, measurable aluminum dissolution was achieved even at low acid concentrations and moderate temperatures (0.1M, 40°C), indicating that leaching can proceed under conditions compatible with electrochemical operation.

Electrochemical testing confirmed that a three-chamber cell with a BPM can generate acid in situ at rates consistent with theoretical predictions. The system exhibited stable operation and rapid acidification of the center chamber, achieving conditions sufficient to support aluminum leaching based on ex situ results.

Future work will focus on integrating solid anorthite directly into the electrochemical cell to evaluate leaching under dynamically generated acid conditions. Additional optimization of membrane selection, electrolyte composition, and operating temperature, and tuning for lunar conditions will further improve system performance and value for ISRU. Ultimately, this approach provides a promising pathway toward reagent-efficient, sustainable metal extraction on the Moon.

Acknowledgements

The first author acknowledges support from the Virginia Space Grant Consortium (VSGC) through a graduate research fellowship.

References

(1) Sanders, G.; Carey, W. C.; Piedboeuf, J.-C.; Lorenzoni, A. LUNAR IN-SITU RESOURCE UTILIZATION IN THE ISECG HUMAN LUNAR EXPLORATION REFERENCE ARCHITECTURE. In *61st International Astronautical Congress*; International Astronautical Federation: Prague, CZ, 2010.

(2) Sanders, G.; Kleinhenz, J. E. Update On NASA ISRU Plans, Priorities, and Activities, 2023.

(3) Sanders, G.; Kleinhenz, J. E. In Situ Resource Utilization (ISRU) Envisioned Future Priorities, 2022.

(4) McKay, D. S.; Heiken, G.; Basu, A.; Blanford, G.; Simon, S.; Reedy, R.; French, B. M.; Papike, J. *The Lunar Regolith*; 1991; pp 285–356.

(5) Anand, M.; Crawford, I. A.; Balat-Pichelin, M.; Abanades, S.; Van Westrenen, W.; Péraudeau, G.; Jaumann, R.; Seboldt, W. A Brief Review of Chemical and Mineralogical Resources on the Moon and Likely Initial in Situ Resource Utilization (ISRU) Applications. *Planet. Space Sci.* **2012**, *74* (1), 42–48. https://doi.org/10.1016/j.pss.2012.08.012.

(6) Taylor, G. J.; Martel, L. M. V.; Lucey, P. G.; Gillis-Davis, J. J.; Blake, D. F.; Sarrazin, P. Modal Analyses of Lunar Soils by Quantitative X-Ray Diffraction Analysis. *Geochim. Cosmochim. Acta* **2019**, *266*, 17–28. https://doi.org/10.1016/j.gca.2019.07.046.

(7) Taylor, S. R. *Lunar Science: A Post-Apollo View: Scientific Results and Insights from the Lunar Samples*; Pergamon Press: New York, 1975.

(8) Schwandt, C.; Hamilton, J. A.; Fray, D. J.; Crawford, I. A. The Production of Oxygen and Metal from Lunar Regolith. *Planet. Space Sci.* **2012**, *74* (1), 49–56. https://doi.org/10.1016/j.pss.2012.06.011.

(9) Schlüter, L.; Cowley, A. Review of Techniques for In-Situ Oxygen Extraction on the Moon. *Planet. Space Sci.* **2020**, *181*, 104753. https://doi.org/10.1016/j.pss.2019.104753.

(10) Schreiner, S. S.; Sibille, L.; Dominguez, J. A.; Hoffman, J. A. A Parametric Sizing Model for Molten Regolith Electrolysis Reactors to Produce Oxygen on the Moon. *Adv. Space Res.* **2016**, *57* (7), 1585–1603. https://doi.org/10.1016/j.asr.2016.01.006.
(11) Shaw, M.; Humbert, M.; Brooks, G.; Rhamdhani, A.; Duffy, A.; Pownceby, M. Mineral Processing and Metal Extraction on the Lunar Surface - Challenges and Opportunities. *Miner. Process. Extr. Metall. Rev.* **2022**, *43* (7), 865–891. https://doi.org/10.1080/08827508.2021.1969390.
(12) Sanders, G. B.; Kleinhenz, J. E.; Boucher, D. Lunar Mining and Processing: Considerations For Responsible Space Mining & Connections to Terrestrial Mining. In *ASCEND 2023*; American Institute of Aeronautics and Astronautics: Las Vegas, Nevada, 2023. https://doi.org/10.2514/6.2023-4621.
(13) Binnemans, K.; Jones, P. T. The Twelve Principles of Circular Hydrometallurgy. *J. Sustain. Metall.* **2023**, *9* (1), 1–25. https://doi.org/10.1007/s40831-022-00636-3.
(14) Mines Canada. *The Canadian Minerals and Metals Plan*; M4-175/2019E; 2019.
(15) Priya, A.; Hait, S. Comparative Assessment of Metallurgical Recovery of Metals from Electronic Waste with Special Emphasis on Bioleaching. *Environ. Sci. Pollut. Res.* **2017**, *24* (8), 6989–7008. https://doi.org/10.1007/s11356-016-8313-6.
(16) Free, M. L. *Hydrometallurgy: Fundamentals and Applications*, 1st ed.; Wiley, 2013. https://doi.org/10.1002/9781118732465.
(17) Davis, K.; Demopoulos, G. P. Hydrometallurgical Recycling Technologies for NMC Li-Ion Battery Cathodes: Current Industrial Practice and New R&D Trends. *RSC Sustain.* **2023**, *1* (8), 1932–1951. https://doi.org/10.1039/D3SU00142C.
(18) Diaz, L. A.; Strauss, M. L.; Adhikari, B.; Klaehn, J. R.; McNally, J. S.; Lister, T. E. Electrochemical-Assisted Leaching of Active Materials from Lithium Ion Batteries. *Resour. Conserv. Recycl.* **2020**, *161*, 104900. https://doi.org/10.1016/j.resconrec.2020.104900.
(19) Pärnamäe, R.; Mareev, S.; Nikonenko, V.; Melnikov, S.; Sheldeshov, N.; Zabolotskii, V.; Hamelers, H. V. M.; Tedesco, M. Bipolar Membranes: A Review on Principles, Latest Developments, and Applications. *J. Membr. Sci.* **2021**, *617*, 118538. https://doi.org/10.1016/j.memsci.2020.118538.
(20) Filingeri, A.; Herrero-Gonzalez, M.; O'Sullivan, J.; Rodriguez, J. L.; Culcasi, A.; Tamburini, A.; Cipollina, A.; Ibañez, R.; Ferrari, M. C.; Cortina, J. L.; Micale, G. Acid/Base Production via Bipolar Membrane Electrodialysis: Brine Feed Streams to Reduce Fresh Water Consumption. *Ind. Eng. Chem. Res.* **2024**, *63* (7), 3198–3210. https://doi.org/10.1021/acs.iecr.3c03553.
(21) De Oca, D. M. M.; Shi, M.; Diaz, L. A.; Lister, T. E. Electrochemical Leaching of Spent LIBs: Kinetics, Novel Reactor, and Modeling. *Sustain. Mater. Technol.* **2024**, *40*, e00898. https://doi.org/10.1016/j.susmat.2024.e00898.
(22) Chernyaev, A.; Partinen, J.; Klemettinen, L.; Wilson, B. P.; Jokilaakso, A.; Lundström, M. The Efficiency of Scrap Cu and Al Current Collector Materials as Reductants in LIB Waste Leaching. *Hydrometallurgy* **2021**, *203*, 105608. https://doi.org/10.1016/j.hydromet.2021.105608.
(23) Golubenko, D. V.; Yaroslavtsev, A. B. Effect of Current Density, Concentration of Ternary Electrolyte and Type of Cations on the Monovalent Ion Selectivity of Surface-Sulfonated Graft Anion-Exchange Membranes: Modelling and Experiment. *J. Membr. Sci.* **2021**, *635*, 119466. https://doi.org/10.1016/j.memsci.2021.119466.

(24) Chatenet, M.; Pollet, B. G.; Dekel, D. R.; Dionigi, F.; Deseure, J.; Millet, P.; Braatz, R. D.; Bazant, M. Z.; Eikerling, M.; Staffell, I.; Balcombe, P.; Shao-Horn, Y.; Schäfer, H. Water Electrolysis: From Textbook Knowledge to the Latest Scientific Strategies and Industrial Developments. *Chem. Soc. Rev.* **2022**, *51* (11), 4583–4762. https://doi.org/10.1039/D0CS01079K.

(25) Mesfin, K. G.; Wolff-Boenisch, D.; Gislason, S. R.; Oelkers, E. H. Effect of Cation Chloride Concentration on the Dissolution Rates of Basaltic Glass and Labradorite: Application to Subsurface Carbon Storage. *Minerals* **2023**, *13* (5), 682. https://doi.org/10.3390/min13050682.

(26) Cheng, H.; Zhang, J.; Lv, H.; Guo, Y.; Cheng, W.; Zhao, J.; Cheng, F. Separating NaCl and AlCl3·6H2O Crystals from Acidic Solution Assisted by the Non-Equilibrium Phase Diagram of AlCl3-NaCl-H2O(-HCl) Salt-Water System at 353.15 K. *Crystals* **2017**, *7* (8), 244. https://doi.org/10.3390/cryst7080244.

(27) Chernyaev, A.; Zhang, J.; Seisko, S.; Louhi-Kultanen, M.; Lundström, M. Fe3+ and Al3+ Removal by Phosphate and Hydroxide Precipitation from Synthetic NMC Li-Ion Battery Leach Solution. *Sci. Rep.* **2023**, *13* (1), 21445. https://doi.org/10.1038/s41598-023-48247-6.

(28) Wang, W.; Jin, Q.; Chen, X.; Jiao, H.; Cai, W.; Lu, Y.; Xu, T.; Wu, Y. Character and Spatial Distribution of Mineralogy at the Lunar South Polar Region. *Planet. Space Sci.* **2024**, *240*, 105833. https://doi.org/10.1016/j.pss.2023.105833.

(29) Lemelin, M.; Lucey, P. G.; Camon, A. Compositional Maps of the Lunar Polar Regions Derived from the Kaguya Spectral Profiler and the Lunar Orbiter Laser Altimeter Data. *Planet. Sci. J.* **2022**, *3* (3), 63. https://doi.org/10.3847/PSJ/ac532c.

(30) Neron, T.; Cassayre, L.; Zhuo, X.; Manero, M.-H.; Bourgeois, F.; Billet, A.-M.; Julcour, C. Thermo-Kinetic Modelling of the Acidic Leaching of Anorthosite: Key Learnings toward the Conception of a Sustainable Industrial Process. *Miner. Eng.* **2022**, *180*, 107500. https://doi.org/10.1016/j.mineng.2022.107500.

(31) PCA GmbH. *Ion Exchange Membranes for Electromembrane Processes: Membrane Handling Guide—Characterisation, Operation and Handling*; PCA GmbH: Heusweiler, Germany, 2021.

(32) Mettler Toledo. *Aluminium in Ground Water; UV/VIS*; Application Note M9122 V1.0; Mettler Toledo, 2022.

(33) *Standard methods for the examination of water and wastewater*, 16th ed.; Greenberg, A. E., Trussell, R. R., Clesceri, L. S., Greenberg, A., American Public Health Association, American Water Works Association, Water Pollution Control Federation, Eds.; American Public Health Association: Washington, D.C, 1985.

(34) Oelkers, E. H.; Schott, J. Experimental Study of Anorthite Dissolution and the Relative Mechanism of Feldspar Hydrolysis. *Geochim. Cosmochim. Acta* **1995**, *59* (24), 5039–5053. https://doi.org/10.1016/0016-7037(95)00326-6.

(35) Addassi, M.; Berno, D.; Afifi, A. M.; Hoteit, H.; Oelkers, E. H. Anorthosite Dissolution as a Function of pH at 60 and 120 °C: Implications for Subsurface Carbon Mineralization. *Carbon Capture Sci. Technol.* **2025**, *15*, 100429. https://doi.org/10.1016/j.ccst.2025.100429.